Phase Shift Calculations for Proton-Proton Scattering at High Energies

H. M. THAXTON* AND L. E. HOISINGTON
University of Wisconsin, Madison, Wisconsin

(Received October 17, 1939)

The theoretical s wave shift for the square well and the Gauss error well which is fitted to experiment from 0.7 to 2.6 Mev is calculated up to energies of 10 Mev. Coulomb functions needed for this purpose are tabulated and the phase shift, as well as the ratio of theoretical scattering to that expected according to Mott's formula, is represented graphically as a function of the energy. The Gauss error well and the square well are found to give very similar extrapolations of the experimental phase shifts to high energies.

ANALYSIS[1, 2] of the experimental data[3] on proton-proton scattering has shown that the p state scattering is small in the energy interval 0.9 to 2.4 Mev. The analysis also shows that on the assumption of pure s state scattering in this energy region the experimental data are closely fitted by the scattering expected from a square potential well of depth 10.50 Mev and range e^2/mc^2 without Coulomb potential inside, or from a Gauss error potential well $Ae^{-\alpha r^2}$ where $A=51.44\ mc^2$ and $\alpha=21.59\ Mmc^2/\hbar^2$, cut off at $r=3e^2/mc^2$ and with Coulomb potential inside. Comparisons with experimental data were also made[2] with the use of square wells of depth 6.3452 Mev and range 1.25 e^2/mc^2, and of depth 19.690 Mev and range 0.75 e^2/mc^2.

The probability that proton-proton scattering experiments will soon be done at energies from 3 to 10 Mev has made it desirable to have the phase shifts and the expected scattering for the above wells calculated for these higher energies. Graphs up to 9 Mev have already been published[2] for the square wells of depth 10.50 Mev and radius e^2/mc^2, and of depth 46.78 Mev and radius 0.5 e^2/mc^2. In this paper the high energy calculations for the others of the above potential wells are reported.

The notation and the values of the physical constants are the same as those used in BTE. The quantities $\Phi_0{}^*/\Phi_0$, $\Phi_0\Theta$ and $C_0{}^2\rho\Phi_0{}^2$ used in the calculation of the phase shift K_0 (BCP Eq. (7.8)) are given in Table I. In the other tables are listed the values of the quantities necessary to find the ratio $\mathfrak{R}$ of the expected scattering to Mott scattering (BTE Eqs. (2.1) and (2.2), and see BCP Eqs. (6) to (6.7)). Tables II, IV and VI give the values of the coefficient of $-\sin K_L \cos K_L$ in the formula for $\mathfrak{R}$ for $L=0$, 1, 2. Tables III, V and VII give the values of the coefficient of $\sin^2 K_L$ for $L=0$, 1, 2. Tables II to VII are extensions of the BCP tables of the same numbers, and Tables II and III are extensions of BTE Tables I and II.

The calculations with the Gauss error potential were made at energy intervals of 1 Mev. The joining to the Coulomb functions was made at $r=3e^2/mc^2$. Interpolations were necessary to obtain the value of $x\mathfrak{F}'/\mathfrak{F}$ at the value of x (here $x=\alpha^{\frac{1}{2}}r$) corresponding to $r=3e^2/mc^2$; these interpolations were made parabolically. At energies of 6 and 7 Mev the value of $x\mathfrak{F}'/\mathfrak{F}$ changes so rapidly with x that interpolations of $\mathfrak{F}$ and $\mathfrak{F}'$ separately were necessary.

Figures 1 to 4 show the phase shifts K_0 for the different potential wells as a function of the energy E of the incident protons. Figs. 1, 2 and 3 illustrate the effects of varying the depths of the square wells of radius 0.75, 1.00 and 1.25 e^2/mc^2 without Coulomb potential inside. Increasing the depth of the well mainly raises the K_0, E curve as a whole, and does not change its shape or slope much. Fig. 4 shows how the shape of the K_0, E curve for the square well without Coulomb potential inside is affected by changing the radius of the well. Decreasing the radius increases the slope and slightly reduces the curva-

* Now at the Agricultural and Technical College of North Carolina.

[1] G. Breit, E. U. Condon and R. D. Present, Phys. Rev. **50**, 825 (1936). This paper will be referred to as BCP.

[2] G. Breit, H. M. Thaxton and L. Eisenbud, Phys. Rev. **55**, 1018 (1939). This paper will be referred to as BTE.

[3] R. G. Herb, D. W. Kerst, D. B. Parkinson and G. J. Plain, Phys. Rev. **55**, 603(A) and 998 (1939); N. P. Heydenberg, L. R. Hafstad and M. A. Tuve, Phys. Rev. **55**, 603(A) (1939). For analysis of the data, see BTE pp. 1035–6.

TABLE I. *Coulomb functions. This table is probably accurate to ±0.02 percent. It is an extension of the table in the appendix of BTE and gives the quantities needed for Eq. (7.8) of BCP.*

E (MEV)	η	$r=0.5\ e^2/mc^2$ Φ_0^*/Φ_0	$r=0.5\ e^2/mc^2$ $\Phi_0\Theta_0$	$r=0.5\ e^2/mc^2$ $C_0^2\rho\Phi_0^2$	$r=0.75\ e^2/mc^2$ Φ_0^*/Φ_0	$r=0.75\ e^2/mc^2$ $\Phi_0\Theta_0$	$r=0.75\ e^2/mc^2$ $C_0^2\rho\Phi_0^2$	$r=e^2/mc^2$ Φ_0^*/Φ_0	$r=e^2/mc^2$ $\Phi_0\Theta_0$	$r=e^2/mc^2$ $C_0^2\rho\Phi_0^2$
3.0	0.091279	1.0005	0.9228	0.2034	0.9829	0.8789	0.3029	0.9530	0.8215	0.3972
3.5	.084508	.9965	.9189	.2239	.9739	.8678	.3319	.9367	.8003	.4324
4.0	.079050	.9925	.9146	.2429	.9649	.8561	.3583	.9204	.7784	.4635
4.5	.074529	.9886	.9098	.2606	.9559	.8439	.3824	.9040	.7562	.4912
5.0	.070704	.9845	.9048	.2772	.9470	.8314	.4047	.8875	.7338	.5161
5.5	.067414	.9806	.8996	.2929	.9377	.8186	.4254	.8708	.7114	.5385
6.0	.064544	.9765	.8942	.3075	.9285	.8057	.4446	.8540	.6890	.5587
6.5	.062012	.9725	.8886	.3215	.9193	.7927	.4625	.8372	.6667	.5770
7.0	.059756	.9685	.8829	.3348	.9101	.7795	.4792	.8202	.6446	.5935
7.5	.057730	.9645	.8771	.3476	.9009	.7663	.4949	.8031	.6225	.6084
8.0	.055897	.9604	.8712	.3597	.8916	.7531	.5096	.7858	.6009	.6219
8.5	.054228	.9564	.8653	.3713	.8823	.7400	.5234	.7685	.5793	.6340
9.0	.052700	.9524	.8593	.3825	.8729	.7268	.5364	.7510	.5583	.6449
9.5	.051294	.9483	.8532	.3932	.8635	.7136	.5486	.7334	.5372	.6547
10.0	.049996				.8541	.7006	.5602			

E (MEV)	η	$r=1.25\ e^2/mc^2$ Φ_0^*/Φ_0	$r=1.25\ e^2/mc^2$ $\Phi_0\Theta_0$	$r=1.25\ e^2/mc^2$ $C_0^2\rho\Phi_0^2$	$r=2\ e^2/mc^2$ Φ_0^*/Φ_0	$r=2\ e^2/mc^2$ $\Phi_0\Theta_0$	$r=2\ e^2/mc^2$ $C_0^2\rho\Phi_0^2$	$r=3\ e^2/mc^2$ Φ_0^*/Φ_0	$r=3\ e^2/mc^2$ $\Phi_0\Theta_0$	$r=3\ e^2/mc^2$ $C_0^2\rho\Phi_0^2$
3.0		0.9108	0.7516	0.4818	0.7004	0.4781	0.6544	0.1728	0.08249	0.6451
3.5		.8851	.7183	.5194	.6282	.4063	.6764	−.03225		.6027
4.0		.8591	.6847	.5515	.5538	.3387	.6880	−.2555	−.07356	.5510
4.5		.8329	.6512	.5791	.4771	.2755	.6914	−.5005		.4942
5.0		.8063	.6179	.6028	.3980	.2169	.6883	−.7715	−.16425	.4359
5.5		.7795	.5851	.6231	.3163	.1623	.6796	−1.0742		.3780
6.0		.7524	.5529	.6404	.2318	.1133	.6666	−1.416	−.2045	.3223
6.5		.7250	.5213	.6550	.1444	.06805	.6500	−1.806		.2700
7.0		.6972	.4904	.6672	.05367	.02701	.6306	−2.259	−.2080	.2219
7.5		.6692	.4601	.6773	−.04038	−.01005	.6089	−2.795		.1784
8.0		.6409	.4306	.6855	−.1382	−.04325	.5854	−3.440	−.1867	.1399
8.5		.6122	.4020	.6919	−.2398	−.07283	.5606	−4.239		.1064
9.0		.5831	.3740	.6967	−.3460	−.09894	.5349	−5.262	−.1498	.07794
9.5		.5537	.3467	.7001	−.4568	−.12187	.5086	−6.627		.05437
10.0		.5241	.3205	.7022				−8.479	−.10579	.03601

ture. Fig. 4 also shows the close agreement of the K_0's as calculated for the square well of radius e^2/mc^2 and depth 10.5 Mev and for the Gauss error well $Ae^{-\alpha r^2}$ with $A=51.44\ mc^2$ and $\alpha=21.59\ Mmc^2/\hbar^2$, the latter potential well being supposed to be superposed on the Coulomb potential. A slight change in the depth and radius of the square well should bring the two curves almost into coincidence. This indicates

TABLE II. *Values of the coefficient (i.e.,* $\mathbf{2X}/\eta\mathfrak{M}$*) of* $-\sin K_0 \cos K_0$ *for* $\mathbf{P}/\mathbf{P}_M$*. This table is an extension of Table I of BTE. For expansions of* $\mathbf{X}$ *and* $\mathfrak{M}$ *in terms of E see BTE Tables III and V.*

E (MEV)	η	$\Theta=15°$	20°	25°	30°	35°	40°	45°
6.0	0.064544	2.348	4.592	8.069	13.23	20.20	27.51	30.96
7.0	0.059756	2.541	4.967	8.722	14.30	21.83	29.72	33.44
8.5	0.054228	2.806	5.482	9.621	15.77	24.06	32.76	36.85
10.0	0.049996	3.050	5.952	10.44	17.10	26.11	35.54	39.98

TABLE III. *Values of the coefficient (i.e.* $4/\eta^2\mathfrak{M}+2\mathbf{Y}/\eta\mathfrak{M}$ *of* $\sin^2 K_0$ *for* $\mathbf{P}/\mathbf{P}_M$*. This table is an extension of Table II of BTE. For expansions of* $2\mathbf{Y}/\eta$ *and* $\mathfrak{M}$ *in terms of E see BTE Tables IV and V.*

E (MEV)	η	$\Theta=15°$	20°	25°	30°	35°	40°	45°
6.0	0.064544	4.225	14.26	36.11	76.17	137.3	205.7	238.7
7.0	0.059756	4.994	16.73	42.26	89.02	160.4	240.2	278.7
8.5	0.054228	6.146	20.44	51.51	108.3	195.1	291.9	338.7
10.0	0.049996	7.303	24.15	60.72	127.6	229.7	343.6	398.7

TABLE IV. *Values of the coefficient of* $-\sin K_1 \cos K_1$ *for* $\mathbf{P}/\mathbf{P}_M$*. Interpolations linear in E may be correct only to about ±0.1 percent.*

E (MEV)	η	$\Theta=15°$	20°	25°	30°	35°	40°	45°
3.0	0.091279	11.34	17.31	21.37	21.16	15.13	5.329	0.000
4.0	0.079050	13.10	19.99	24.67	24.43	17.46	6.122	0.000
5.0	0.070704	14.66	22.36	27.58	27.30	19.51	6.841	0.000
7.0	0.059756	17.35	26.45	32.67	32.30	23.07	8.090	0.000
10.0	0.049996	20.75	31.62	38.99	38.59	27.56	9.664	0.000

TABLE V. *Values of the coefficient of* $\sin^2 K_1$ *for* $\mathbf{P}/\mathbf{P}_M$*. Interpolations linear in E are very good.*

E (MEV)	η	$\Theta=15°$	20°	25°	30°	35°	40°	45°
3.0	0.091279	45.69	116.4	205.3	260.0	218.6	84.38	0.000
4.0	0.079050	61.27	155.8	273.7	346.8	291.5	112.5	0.000
5.0	0.070704	76.85	195.0	342.3	433.6	360.1	140.6	0.000
7.0	0.059756	108.0	273.4	479.6	607.1	510.3	196.8	0.000
10.0	0.049996	154.8	390.8	685.8	867.5	729.1	281.1	0.000

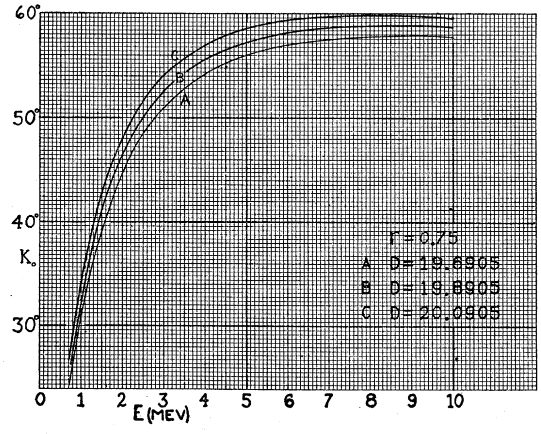

FIG. 1. The phase shift K_0 as a function of the energy E of the incident protons for square potential wells of radius 0.75 e^2/mc^2 and depths 19.690, 19.890 and 20.090 Mev without interior Coulomb potential.

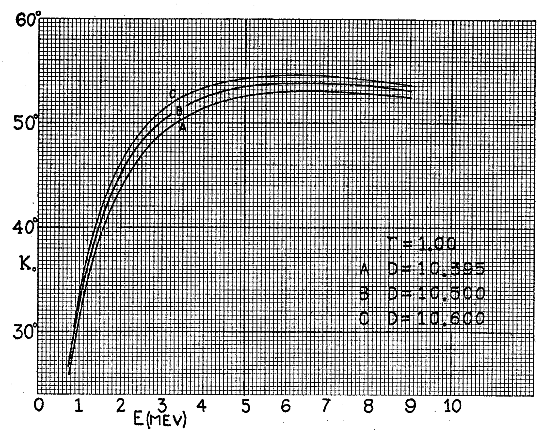

FIG. 2. The phase shift K_0 as a function of the energy E for square wells of radius e^2/mc^2 and depths 10.305, 10.50 and 10.60 Mev without interior Coulomb potential.

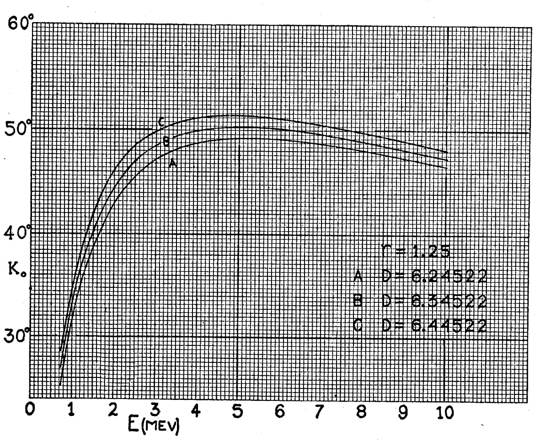

FIG. 3. The phase shift K_0 as a function of the energy E for square wells of radius 1.25 e^2/mc^2 and depths 6.2452, 6.3452 and 6.4452 Mev without interior Coulomb potential.

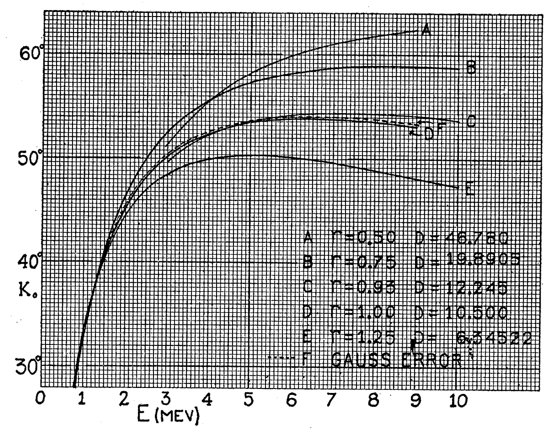

FIG. 4. The phase shift K_0 as a function of the energy E for square wells of differing radii (r is in e^2/mc^2). The depth (in Mev) is adjusted for each radius so as to give coincidence with the experimental K_0 at approximately 1.4 Mev. There is no interior Coulomb potential. The broken line F is for the Gauss error potential well $Ae^{-\alpha r^2}$, where $A=51.44$ mc^2 and $\alpha=21.59$ $Mmc^2/\hbar^2$, cut off at $r=3e^2/mc^2$ and with interior Coulomb potential.

that the high energy region will not be more useful than the low energy region in distinguishing between the two types of potential wells by means of the s wave phase shift.

Figure 5 shows how the ratio $\mathcal{R}$ of theoretical scattering to Mott scattering varies with the energy and the scattering angle. The curves for the square well of depth 10.5 Mev and radius e^2/mc^2 lie very close to those for the Gauss error well.

The curves in Figs. 6 and 7 show the theoretical number of proton counts as a function

TABLE VI. *Values of the coefficient of $-\sin K_2 \cos K_2$ for $\mathbf{P}/\mathbf{P}_M$. Interpolations linear in E may be correct only to about ± 0.1 percent.*

E (Mev)	η	$\Theta=15°$	20°	25°	30°	35°	40°	45°
3.0	0.091279	5.241	6.177	3.390	−5.764	−22.78	−43.35	−53.57
4.0	0.079050	6.060	7.150	3.929	−6.686	−26.44	−50.33	−62.21
5.0	0.070704	6.780	8.005	4.402	−7.495	−29.65	−56.46	−69.78
7.0	0.059756	8.029	9.486	5.221	−8.896	−35.20	−67.05	−82.88
10.0	0.049996	9.602	11.35	6.251	−10.66	−42.17	−80.37	−99.34

TABLE VII. *Values of the coefficient of $\sin^2 K_2$ for $\mathbf{P}/\mathbf{P}_M$. Interpolations linear in E are very good. (For the calculation of d scattering there is a third term, which is $+(40/\eta^2)\sin K_0 \sin K_2 \cos[K_2-K_0+2\sigma_2-2\sigma_0]$. See BCP Eq. (6.7).)*

E (Mev)	η	$\Theta=15°$	20°	25°	30°	35°	40°	45°
3.0	0.091279	22.72	27.37	7.085	14.03	177.8	525.9	738.7
4.0	0.079050	30.23	36.31	9.290	19.06	238.6	704.4	988.7
5.0	0.070704	37.74	45.26	11.498	24.08	299.4	882.8	1238.7
7.0	0.059756	52.77	63.14	15.91	34.12	421.0	1239.6	1739
10.0	0.049996	75.31	89.97	22.53	49.19	603.4	1775	2489

of the energy of the incident protons. The number given is the number expected from the scattering chamber used by Herb, Kerst, Parkinson and Plain[3] per microcoulomb of incident proton current per mm of oil hydrogen pressure in the chamber. Fig. 6 is for the square well of depth 19.690 Mev and radius 0.75 e^2/mc^2 without interior Coulomb potential; added as broken lines are the curves for the Gauss error potential well $Ae^{-\alpha r^2}$, where $A=51.44$ mc^2 and $\alpha=21.59$ $Mmc^2/\hbar^2$, with interior Coulomb potential. Fig. 7 is for the square well of depth 6.3452 Mev and radius 1.25 e^2/mc^2 without interior Coulomb potential; the dotted lines are the same Gauss error curves as in Fig. 6. For a similar graph for square wells of radius 0.5 and 1.0 e^2/mc^2 see BTE Fig. 14. In each case pure s state scattering is assumed.

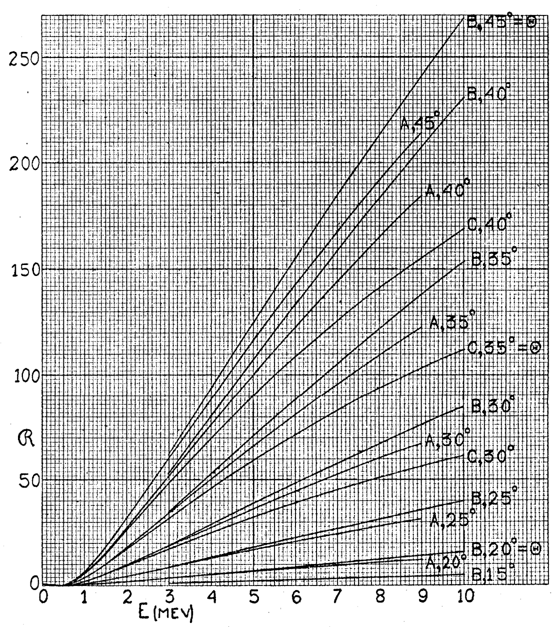

FIG. 5. The ratio ℛ to Mott scattering, as a function of the energy E and the scattering angle Θ, of the scattering calculated for: A, Gauss error well $Ae^{-\alpha r^2}$, where $A=51.44$ mc^2, and $\alpha=21.59$ $Mmc^2/\hbar^2$; B, square well of radius 0.75 e^2/mc^2 and depth 19.690 Mev, and C, square well of radius 1.25 e^2/mc^2 and depth 6.3452 Mev. The curves for a square well of depth 10.50 Mev and radius e^2/mc^2 would lie very close to A.

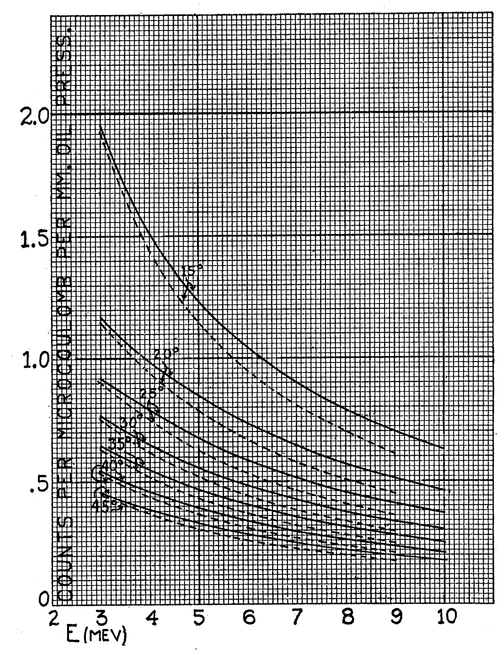

FIG. 6. The number of proton counts expected plotted as a function of the energy E of the incident protons and as a function of the scattering angle Θ. The unbroken curves are for the square well of radius 0.75 e^2/mc^2 and depth 19.690 Mev without interior Coulomb potential. The broken-line curves are for the Gauss error well $Ae^{-\alpha r^2}$, where $A=51.44$ mc^2, and $\alpha=21.59$ $Mmc^2/\hbar^2$ with interior Coulomb potential. For curves for the square well of radius e^2/mc^2 and depth 10.50 Mev, see BTE Fig. 14. The number plotted is the number of counts expected from the scattering chamber of HKPP[3] per microcoulomb of incident proton current per mm of oil hydrogen pressure in the scattering chamber (see BTE). Pure s state scattering is assumed.

Figures 6 and 7 show that the sensitivity of the number of counts to a change in the range of nuclear force is no greater at higher energies than at energies below 3 Mev. (It must be remembered that the energy of the point of intersection of two phase shift curves for different ranges of force is determined by the depth of the wells.) For the larger values of the scattering angle Θ experiments at energies from 1 to 3 Mev may be best for determining the range of the well. (See BTE Fig. 14 and discussion on p. 1059 regarding small angle scattering.) Thus it appears that as far as the s state scattering is concerned

TABLE VIII. *Values of K_1 for the constant potential ± 10.5 Mev of radius e^2/mc^2.*

Energy of incident protons (Mev)	3	4	5	6	7	8	9	10
K_1 (attractive potential)	0.40°	0.63°	0.90°	1.1(9)°	1.5(4)°	1.8(7)°	2.2(3)°	2.6(1)°
K_1 (repulsive potential)	−0.23°	−0.36°	−0.51°	−0.67°	−0.85°	−1.0(4)°	−1.2(3)°	−1.4(2)°

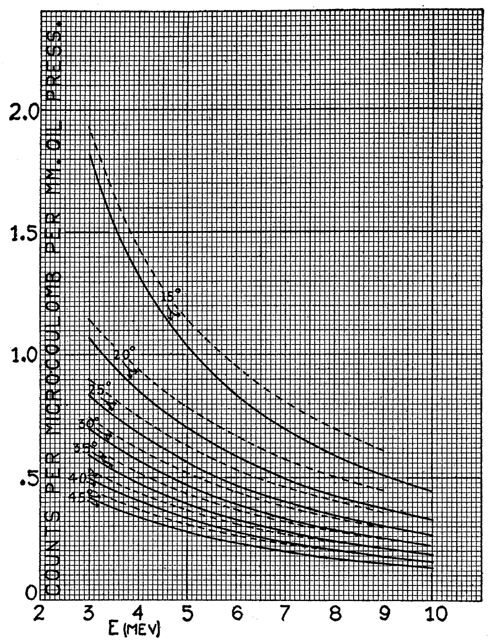

FIG. 7. The same type of curve as Fig. 6. The unbroken curves are for a square well of radius 1.25 e^2/mc^2 and depth 6.3452 Mev. The broken-line curves are the same as in Fig. 6.

the chief value of high energy experiments will be to corroborate the results of the low energy experiments and to make possible better determinations of the range and depth of the potential well by increasing the length of the K_0, E curve to be fitted by theory. The determination of K_0 may be more complicated because of the presence of phase shifts K_1 and K_2.

The experiments at energies above 3 Mev are, however, expected to be very valuable in determining the p state interaction (see BTE pp. 1059–61). In Table VIII are given values of the phase shift K_1 calculated for a constant potential of ± 10.5 Mev with a range of e^2/mc^2 and without interior Coulomb potential. The second and third rows of the table correspond, respectively, to attractive and repulsive p interactions. In both cases it is seen that the absolute values of K_1 increase with energy as would be expected. For the Gauss error potential $\pm Ae^{-\alpha r^2}$ with $A = 51.44\ mc^2$ and $\alpha = 21.59\ Mmc^2/\hbar^2$ superposed on the Coulomb potential, one finds, by integrating the wave equation numerically and joining to the Coulomb function at $r = 3\ e^2/mc^2$, that for a repulsive p state interaction $K_1 = -0.74°$ at 5 Mev, while for an attractive interaction $K_1 = +1.23°$ at the same energy. These values are larger than the corresponding values for the constant potential because the Gauss error potential extends to larger values of r. Beyond showing that the values of K_1 are probably large enough to appear in high energy scattering experiments, these values of K_1 have little direct significance, since it is improbable that the singlet s state and triplet p state interactions are the same.

If the Coulomb potential is considered to be effective inside a square potential well, the depth of the well must be increased in compensation if one wishes to obtain the same phase shift K_0 as was obtained without the interior Coulomb potential. The necessary increase in depth of the square well of depth 10.5 Mev and radius e^2/mc^2 was found to be 0.849 Mev at the energy 7 Mev, and 0.860 Mev at the energy 10 Mev. The calculations were made by the use of BTE Eq. (11.2) and checked by BTE Eq. (11.5). It may be noted that, as a very rough empirical rule, $\delta D = 0.826 + 0.00333\ (E - 0.2)$, for this well, where δD and E are in Mev.

The authors are glad to express their thanks to Professor G. Breit for very helpful discussion and advice.